Exp Brain Res (1999) 125:353–364

RESEARCH ARTICLE

Dianne M. Broussard · Jotinder K. Bhatia
Gavin E.G. Jones

The dynamics of the vestibulo-ocular reflex after peripheral vestibular damage

I. Frequency-dependent asymmetry

Received: 21 January 1998 / Accepted: 1 October 1998

Abstract Accurate performance by the vestibulo-ocular reflex (VOR) is necessary to stabilize visual fixation during head movements. VOR performance is severely affected by peripheral vestibular damage; after one horizontal semicircular canal is plugged, the horizontal VOR is asymmetric and its amplitude is reduced. The VOR recovers partially. We investigated the limits of recovery by measuring the VOR's response to ipsilesional and contralesional rotation after unilateral peripheral damage in cats. We found that the VOR's response to rotation at high frequencies remained asymmetric after recovery was complete. When the stimulus was a pulse of head velocity comprising a dynamic overshoot followed by a plateau, gain was partially restored and symmetry completely restored within 30 days after the plug, but only for the plateau response. The overshoot in eye velocity remained asymmetric. The asymmetry was independent of stimulus velocity throughout the known linear velocity range of primary vestibular afferents. Sinusoidal rotation at 0.05–8 Hz revealed that, within this range, the persistent asymmetry was significant only at frequencies above 2 Hz. Asymmetry was independent of the peak head acceleration over the range of 50–500°/s^2. When both horizontal canals were plugged, a small residual VOR was observed, suggesting residual signal transduction by plugged semicircular canals. However, transduction by plugged canals could not explain the enhancement of the VOR gain, at high frequencies, for rotation away from the plugged side compared with rotation toward the plug. Also, the high-frequency asymmetry was present after recovery from a unilateral labyrinthectomy. These results suggest that high-frequency asymmetry after unilateral damage is not due to residual function in the plugged canal. The findings are discussed in the context of a bilateral model of the VOR that includes central filtering.

Key words Vestibulo-ocular reflex · Vertigo · Labyrinthectomy · Compensation · Motor learning · Oculomotor · Plasticity · Cat

D.M. Broussard (✉) · J.K. Bhatia
Playfair Neuroscience Unit, University of Toronto, MC12–409, The Toronto Hospital, Western Division, 399 Bathurst St., Toronto, Ontario, Canada M5T 2S8
e-mail: dianne@playfair.utoronto.ca
Tel.: +1-416-603-5435, Fax: +1-416-603-5745

D.M. Broussard · G.E.G. Jones
Department of Physiology, University of Toronto, Toronto, Ontario, Canada

Introduction

The vestibulo-ocular reflex (VOR) keeps ocular fixation stable during head movements by rotating the eyes to counteract rotation of the head. One measure of VOR performance is its gain, the ratio of the eye velocity generated by the reflex to the head velocity that drives it. After damage to one vestibular labyrinth, VOR gain is reduced, particularly for rotation toward the damaged side. In addition to the loss of gain and dynamic asymmetry, a superimposed drift or slow phase of nystagmus may make the VOR appear asymmetric. The gain of the VOR increases toward normal over a period of days or weeks following unilateral damage (Courjon et al. 1977; Maioli et al. 1983; Paige 1983; Fetter and Zee 1989a). For head velocities exceeding 100°/s (Baloh et al. 1979; Paige 1983; Fetter and Zee 1989a; Tusa et al. 1996) or sudden accelerations exceeding 1000°/s^2 (Halmagyi et al. 1993; Tabak and Collewijn 1995; Aw et al. 1996; Foster et al. 1997), the VOR may not regain its symmetric response to rotation, even months or years postlesion.

Recently, a slight persistent asymmetry after unilateral damage has been observed at frequencies of rotation above 1 Hz (Vibert et al. 1993; Foster et al. 1997). The persistent asymmetry may be related to stimulus frequency *per se*, perhaps due to limitations imposed by signal transmission in the central VOR pathway. Or the asymmetry may depend only on rotational velocity and acceleration, since rotational acceleration increased with stimulus frequency. The nonlinear responses of primary

afferents at high rotational velocities are generally held responsible for the failure of the VOR to recover its symmetry after unilateral damage ("Ewald's second law"). For example, the VOR shows persistent asymmetric responses to rapid accelerations in vestibular patients (Halmagyi et al. 1993; Foster et al. 1997) as well as other persistent defects (Fetter et al. 1990). After unilateral damage, the response of the VOR and other reflexes would be expected to reflect the properties of the afferents from the intact labyrinth. However, in the 1- to 10-Hz range, canal primary afferents encode a combination of angular velocity and acceleration (Fernandez and Goldberg 1971; Lisberger and Pavelko 1986) and show linear responses over a wide range of velocity and acceleration (Fernandez and Goldberg 1971; Goldberg and Fernandez 1971a). Within the linear range of primary afferents, other factors such as the nonlinearities in the central VOR circuitry and limitations of visually guided recovery may contribute to persistent asymmetry.

The recovery of VOR gain after hemilabyrinthectomy or neurectomy reflects several concurrent processes, such as the gradual recovery and/or loss of afferent activity (Jensen 1983; Gacek et al. 1992; Yamane et al. 1995), learning guided by retinal slip (Ito 1972; Gonshor and Melvill Jones 1973; Miles and Evarts 1979), and correction of any nystagmus (Courjon et al. 1977; Paige 1983; Fetter and Zee 1989a). Visually guided mechanisms are thought to play an important part in the VOR's recovery after peripheral damage (Courjon et al. 1977; Paige 1983; Fetter and Zee 1989b), but other physiological processes may be triggered by the occurrence of injury (Cirelli et al. 1993). Some, although probably not all, of these mechanisms are also expected to be involved in recovery of dynamic symmetry after a plug.

In this paper we describe the response of the VOR at frequencies up to 8 Hz and attempt to determine what factors limit the recovery of dynamic symmetry. Some of the results reported here have been published in abstract form (Broussard and Bhatia 1994, 1996).

Materials and methods

Measurement of eye movements

Five juvenile cats (aged 4–7 months at the start of experiments) and one adult cat (cat G) were used for these experiments. NIH guidelines for the care and use of laboratory animals were followed throughout. For recording, the cats were loosely restrained, lying prone with head upright, in a drawstring bag inside a box. Cats were conditioned using a food reward to enter the bag voluntarily and accept the restraint. After conditioning, a head holder and eye coil were implanted as follows: The cat was premedicated with a mixture of Demerol (3 mg/kg), acepromazine (0.7 mg/kg), and atropine (30 μg/kg) given i.m., anesthetized with isoflurane, intubated, respirated, and placed in a stereotaxic apparatus. Heart rate was monitored and 0.9% saline was given intravenously throughout anesthesia, which was maintained with 1–3% isoflurane. A single midline incision was made and the skin and muscle retracted. The periosteum was left intact to the extent possible. Three veterinary fixation plates (Synthes Canada) were attached to the skull by stainless steel self-tapping cortical screws. The head-holder socket, a stainless steel cylinder, was cemented to the plates.

Eye movements were recorded using the magnetic search coil method. To implant the eye coil, the nictitating membrane was first retracted using 1% Neo-Synephrine. The conjunctiva was dissected away from the globe and four fine sutures attached to the sclera to allow manipulation of the globe. A prefabricated eye coil, 17–20 mm in diameter, was fitted to the eye and attached using the sutures. The cornea was irrigated regularly during surgery. Buprenorphine (30 μg), an analgesic, was given postoperatively.

For recording, field coils (Remmel Labs) generated horizontal and vertical alternating magnetic fields at different frequencies. The signal induced in the eye coil was separated into horizontal and vertical components that were electronically filtered using second-order low-pass filters, with a rolloff at 500 Hz, and digitized by a Pentium-based computer. Data acquisition, as well as subsequent analysis and the model simulations, was carried out using the Labview engineering software package (National Instruments). The sampling rate depended on the stimulus that was being used: For velocity pulses, all channels were sampled at 1000 Hz. For frequencies f of 0.65 Hz and higher, the sampling rate was $200 \times f$. For $f < 0.65$ Hz, the sampling rate was 130 Hz. All channels were digitally filtered with a stopband of 55–65 Hz using a second-order virtual Butterworth filter (National Instruments). Horizontal and vertical angular eye position were calculated and differentiated digitally. Eye and head velocity signals were then low-pass-filtered using second-order virtual Butterworth filters with a rolloff at 50 Hz. The Remmel magnetic coil system was left continuously on and the calibration checked daily, using an eye coil identical to those implanted in the cats, attached to a protractor. The eye coil worn by each cat was calibrated after implantation by rotating the cat and field coils on a rate table at a constant velocity for 500 ms or 1000 ms. Lights were on and an assistant stood in front of the cat. Eye velocity was assumed to equal head velocity during the steady state. This procedure required adjustments of less than 10% from the protractor calibration.

While recording eye movements in darkness, we ensured that the cat remained alert. An assistant remained in the recording cubicle with the cat and provided a variety of interesting sounds. In cats C, D, G, and K we administered 0.5 mg/kg amphetamine when necessary to prevent drowsiness. Amphetamine reduced the variability in our measurements of VOR gain, particularly at high frequencies. VOR gain and phase were not affected in any systematic way by amphetamine at dosages up to 1 mg/kg.

Vestibular stimulation

For measurements of the VOR, the cat was in complete darkness in a closed recording room. The cat's head was immobilized in the stereotaxic (upright) position for most recordings. In one set of experiments, the pitch angle of the head was varied with respect to the earth-vertical axis of rotation by means of a joint in the superstructure that permitted rotation around the interaural axis. We were able to vary the pitch angle from 10° nose-up to 40° nose-down from upright, without causing discomfort to the cat.

Rotation around an earth-vertical axis was generated by a 30 ft.-lb. velocity servo-controlled turntable (Neurokinetics). The tachometer output was digitized to monitor head velocity. Angular velocity commands were (1) short velocity pulses and (2) sinusoids. Velocity pulses were used to evaluate VOR function because others have shown, using impulsive testing, that the VOR is asymmetric in some patients. During velocity pulses, the actual table velocity had a 90-ms rise time, followed by an overshoot that equalled 1.25 times the steady state. This underdamped velocity profile was used because it revealed interesting characteristics of the VOR. Velocity pulses needed to be as long as possible, to allow time for the velocity to approach a true steady state. However, pulses above a particular duration and velocity (which varied among individuals) yielded a consistent quick phase during the pulse. In cat C, we used a relatively long pulse (500 ms) to improve the approximation of steady state, but a quick phase nearly

always occurred by the end of the pulse. In the other cats, we chose a standard pulse for each cat that was as long as possible without quick phases. The standard pulse duration was 250 ms in cats H and P and 300 ms in cats D and K. The standard pulse steady-state velocity was 10°/s in cat D, 20°/s in cats C, K, and H, and 30°/s in cat P. Corresponding peak velocities were 12.5°/s, 25°/s, and 37.5°/s. Rightward and leftward pulses were delivered in a pseudorandom sequence, with onsets separated by 1 s (for 250- and 300-ms stimuli) or 2 s (for 500-ms stimuli).

Sinusoidal stimuli ranged in frequency from 0.05 to 8 Hz. At each frequency, 30 or 40 cycles were acquired, except at 0.05 Hz, where 18 cycles were acquired. The first cycle after the start of rotation was not saved. Frequency was varied at a peak velocity of 10°/s. Peak acceleration and velocity were monitored and the command signal adjusted when necessary to compensate for the dynamics of the apparatus. In general, head velocity was assumed to equal turntable velocity, as was the case for all responses reported here (but see below).

Artifacts in VOR recordings can be generated by relative motion of the cat's head and the field coils, due either to torsion of the coupling between the head and the frame or to flexion of the field coils or superstructure. In preliminary tests, we first looked for any signal generated by flexion of the field coils by gluing a coil to the head-holder post. No signal was generated at frequencies up to 15 Hz using this method. The possible contribution of deformation of the superstructure to our recordings was tested using a mechanical mockup consisting of a search coil glued to a 300-g cube of wood and attached to the superstructure by a standard head holder. We also recorded the eye coil signal during rotation in a deeply anesthetized cat. At 10 Hz and higher frequencies, some relative motion of the head or head mockup and the field coils did occur. Signals corresponding to a "gain" of approximately 0.1 at 10 Hz were generated both by the anesthetized cat and by the mechanical mockup. For sinusoids at 8 Hz or below (peak velocity, 10°/s) and velocity pulses, relative motion was not detectable in either case. Since the results reported here were obtained at 8 Hz or lower frequencies, it is unlikely that artifacts are present in our results. Testing with the mechanical mock-up was repeated at intervals throughout the experiments.

Horizontal canal plug and labyrinthectomy

Before plugging the horizontal canal or removing the labyrinth on one side, we obtained baseline data using the above stimuli. Then, cats were anesthetized and, using a dorsal approach, the temporal bone was exposed. After exposing the head of the incus as a landmark, we drilled the labyrinthine bone away over the horizontal canal, opening the lateralmost portion of the canal for 2–3 mm. The canal was quickly plugged at both ends of the opening with small pieces of periosteum. Plugging was considered complete when there was no leakage of endolymph. For labyrinthectomies, all three semicircular canals, the sacculus, and the utriculus were opened with the burr and all soft tissue removed. Cats were given 30 μg buprenorphine postoperatively (buprenorphine alone had no effect on the VOR).

The horizontal semicircular canal was plugged on the left side in cat D and on the right side in cats C, H, P, and Z. In cat C, the posterior canal was plugged on the right side during the same operation. In cat K, the left labyrinth was removed. Both horizontal canals were plugged in a single operation in G. In cat D, the second horizontal canal was plugged after the postrecovery data had been obtained. We will refer to each cat by the identifying letter followed by the condition under which data were obtained: either NRM (normal), CP or BCP (unilateral or bilateral canal plug), or LBX (unilateral labyrinthectomy).

Cats had access to a large play area for several hours per day and were encouraged to run and jump during the recovery period. The first postoperative data point was obtained from cat K 72 h after the labyrinthectomy. In the other cats, recording was begun on the morning after the canal plug. The VOR was recorded once or more per day for 1 week, 2–3 times a week for 8 weeks or more, and at longer intervals for up to 4 months after the plug. Postmortem dissection revealed that plugged cats had complete bony occlusion of the horizontal canal.

Analysis of velocity pulses

All data were analyzed using the Labview package (National Instruments). For velocity pulses, the horizontal eye and head velocity records in each direction were averaged together; records containing saccades were discarded. Records with quick phases were discarded for the standard velocity pulse in all cats except C, because quick phases consistently occurred only in cat C. This was because the standard pulse duration was 300 ms or less in all of the other cats, but 500 ms in cat C. For 500-ms pulses of 20°/s or higher and 250-ms pulses of 40°/s or higher, quick phases were removed and replaced with a straight-line segment. In general, if the removal caused apparent distortion of the response, it was excluded from the mean. In cat C, the removal of quick phases near the end of each pulse resulted in artificially increased "undershoots" after the pulse in the averaged traces. These artifacts were included in the means because they did not affect the measured values of gain or dynamic index. However, they did affect the outcome of power spectral analysis. Therefore, data from cat C were not used in spectral analysis.

Figure 1 illustrates the peak and plateau of the response to a velocity pulse. Peak eye velocity was determined automatically. The plateau was more difficult and crucial to define correctly because of ringing. The bias introduced by the ringing was minimized by choosing the plateau so that any maxima were counterbalanced by minima. Thus, the plateau was a period, 100 ms or more, of relatively constant eye velocity during which eye velocity was distributed equally on both sides of the mean. The plateau gain was defined as the ratio of the mean eye and head velocities during the plateau. The dynamic index was defined as

$$DI = \frac{E'_{pk}}{(\sum_{i=m}^{m+n} E'_i)/(n+1)}$$

where E'_{pk} is peak eye velocity, n is the number of data points assigned to the plateau (indicated in Fig. 1), and m is the index of the first point assigned to the plateau. The dynamic index is a very coarse indicator of the frequency response of the system over a limited frequency range, and has the advantage of being independent of the overall gain of the system. Because of the overshoot in head velocity, the dynamic index refers to the response of the entire system including the turntable. Therefore, we use it here as a relative measure in different situations.

After a unilateral canal plug, cats showed no nystagmus and little or no drift toward the plugged side. If a slight drift was present, it was measured by averaging 50–170 ms of eye velocity data before the beginning of the rotation, and subtracted from the peak and plateau eye velocity. After a unilateral labyrinthectomy, cat K(LBX) showed nystagmus as expected. We did not attempt to measure VOR gain in cat K until the nystagmus had resolved. Single exponentials of the form

$$f = 0.4 + C/(1 - e^{-ax})$$

were fit to the time course of the plateau gain during recovery from a plug. The value of 0.4, or one-half of the mean VOR gain in our normal cats, represented VOR gain immediately after the unilateral plug.

The power spectrum of the velocity pulse was computed in order to determine whether or not the frequency range of the sinusoidal stimuli was adequate to investigate the asymmetry we had observed with pulses. A transfer function, over the range of frequencies employed here, was computed as the ratio of the cross power spectrum of stimulus and response to the power spectrum of the stimulus.

Analysis of sinusoids

For the sinusoidal VOR at 1–8 Hz, the first positive-going zero crossing was identified and succeeding cycles were averaged, rejecting any cycles that contained saccades. Quick phases were not present owing to the small amplitude of the stimulus (0.4–3.2° peak to peak). At 0.5 Hz and 0.05 Hz, quick phases were removed and replaced with straight-line segments before averaging. Then, sinusoids at the driving frequency were fit, using a modified Levenberg-Marquardt (nonlinear) least-squares regression, to the eye and head velocity means. The phase of the VOR was defined as the angle by which the best fit to eye velocity led the best fit to head velocity; phase lags were negative. The gain of the VOR was defined as the ratio of the peak amplitudes of the fitted sinusoids.

The asymmetric response of the VOR to sinusoids after recovery from a plug was quantified as follows: A sinusoid was fit to the eye velocity curve. The ipsiversive and contraversive responses were defined as the half-cycles surrounding each peak in the fitted curve. The curve was shifted along the velocity axis until the half-cycles began and ended at zero, if necessary (it usually was not); this step eliminated any bias velocity. The half-cycles were then duplicated and inverted. Half-cycles and their inverted duplicates were combined to simulate "full cycles" of either ipsilesional or contralesional rotation. The full cycles were fit with a sinusoid at the driving frequency (for example, see Fig. 6).

Results

The response of the normal VOR to velocity pulses

The top traces in Fig. 1 illustrate the response of the VOR in a normal cat to a pulse of angular velocity with a 500-ms duration, a plateau velocity of 20°/s, and a mean acceleration during the rising phase of 304°/s^2. In this and other figures, rightward head and eye velocity are positive. Head velocity pulses showed overshoot and ringing at the resonant frequency of the turntable. This underdamping improved the bandwidth of the stimulus and was advantageous for our experiments. Eye velocity followed head velocity with a similar time course, except for a slight decline during the plateau of 500-ms pulses. We calculated the ratio of mean eye to head velocity during the plateau ("plateau gain") and the ratio of the peak velocity to the plateau velocity for eye and head ("dynamic index"). Distributions of plateau gain and dynamic index for eye velocity are shown for four cats in Fig. 1 (middle panel). The gain of the VOR was approximately 0.8, and the dynamic index in the normal cat was about 1.35. These parameters were relatively constant across individuals. None of our cats showed any significant asymmetry in gain or dynamic index before the plug. The dynamic index for head velocity was also greater than 1 owing to turntable dynamics. Means and standard deviations of the dynamic index for head velocity, for all four cats, are shown in Fig. 1 (lower panel); the mean value was approximately 1.25. The turntable dynamics represented in the lower panel clearly contributed to the eye dynamic index shown in the middle panel; in other words, the eye dynamic index was not the true dynamic index of the VOR. The eye dynamic index was useful primarily for comparisons between reponses to leftward and rightward rotations, and for comparisons between normal and postsurgical conditions, in the same cat.

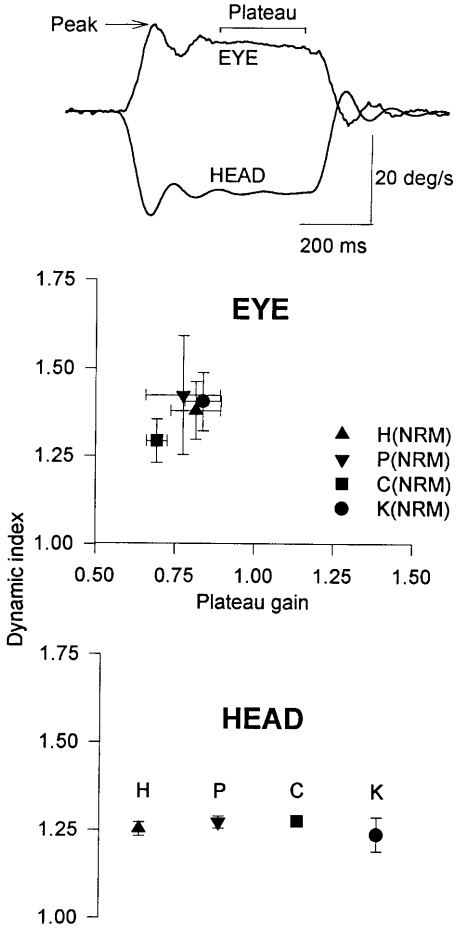

Fig. 1 Response of the normal VOR to pulses of horizontal angular velocity. *Top*: Head and eye velocity during a pulse with a 500-ms plateau. Twelve responses were averaged. Rotation was leftward in this example. *Center*: Means and standard deviations of plateau gain and dynamic index for eye velocity, recorded on different days. Values for leftward and rightward rotations were averaged together. Data were recorded on 14 presurgical days in cat P(NRM), 20 days in cat H(NRM), 23 days in cat C(NRM), and 6 days in cat K(NRM). *Bottom*: Means and standard deviations of dynamic index for head velocity for the same four cats. Pre- and postsurgical data were pooled. Sample sizes were 26 for cat H, 39 for P, 40 for cat C, and 16 for cat K

The time course of recovery from a unilateral plug

Figure 2 illustrates the time course of recovery of the gain and symmetry of the VOR after a unilateral horizontal canal plug. On postoperative day 1, the plateau gain of the VOR was approximately half of normal; some cats also had a slow ipsilesional drift ranging from 0.5 to 11°/s in darkness. Any drift was subtracted before measuring VOR gain. The plateau gain recovered rapidly toward an asymptote, with similar time courses for ipsi- and contralesional rotation. Individual data points are shown in Fig. 2 for cat P(CP). The time course of recov-

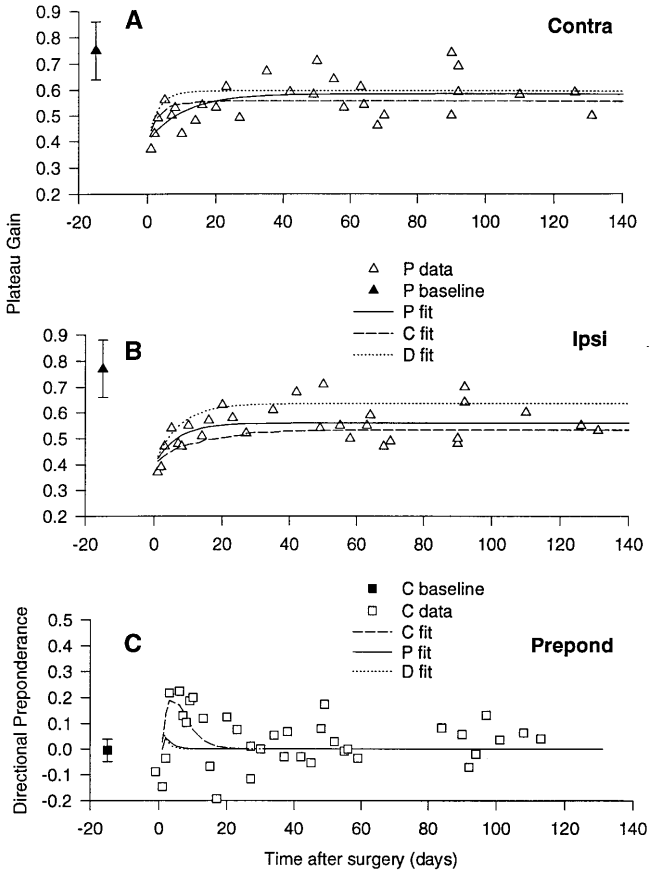

Fig. 2A–C Time course of recovery of plateau gain after a unilateral canal plug. Curves are single exponentials fit to the data for each cat. **A** Response to contralesional rotation. **B** Ipsilesional rotation. Symbols in **A** and **B** are data points from individual days after the canal plug for cat P(CP). Means and standard deviations of plateau gains before the plug are also shown for cat P(NRM; P baseline; *n*=14). **C** Directional preponderance. Symbols are data points for cat C(CP). Mean and standard deviation of preponderance before the plug are shown for cat C(NRM) (*n*=22)

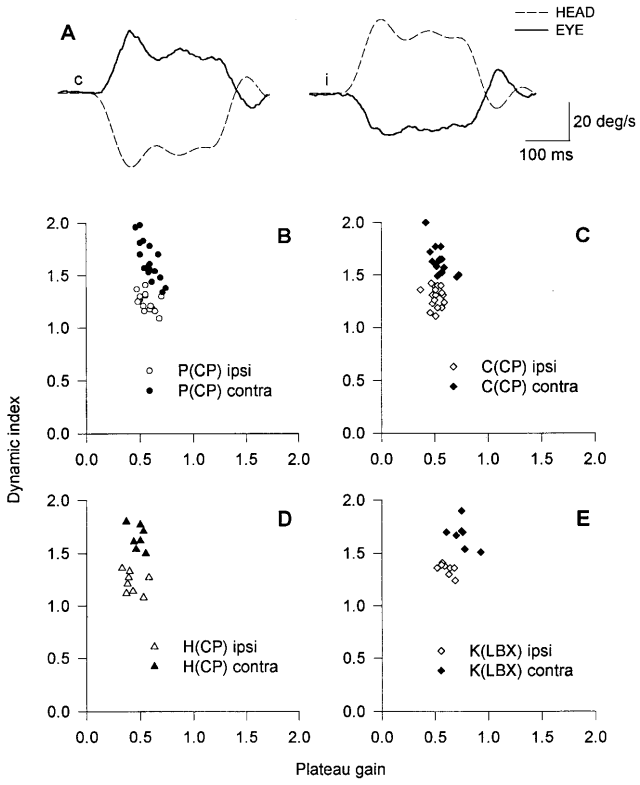

Fig. 3A–E Response to velocity pulses after recovery from a canal plug or labyrinthectomy. **A** Head and eye velocity of cat P during ipsi- and contralesional rotation on day 35 after the canal plug. Data from cat P(CP) are shown in **B**, from cat C(CP) in **C**, from cat H(CP) in **D**, and from cat K(LBX), the hemilabyrinthecomized cat, in **E**. Each point represents gain and dynamic index for either ipsilesional (*empty symbols*) or contralesional (*filled symbols*) rotation on a given day. All measurements were made between 30 and 131 days postlesion

ery from a plug in each cat was fit by a single exponential curve with a time constant between 3 and 10 days. The asymptote was approximately 70% of the normal gain. We could not demonstrate an increase in gain more than 30 days after the plug for any of our cats, and we considered data obtained more than 30 days after surgery to be "after recovery."

Recovery was slightly more rapid for contralesional (Fig. 2A) than for ipsilesional rotation (Fig. 2B), resulting in a transient asymmetry. Asymmetry in the VOR can be represented by directional preponderance (DP), defined as

$$DP = \frac{G_{contra} - G_{ipsi}}{G_{contra} + G_{ipsi}}$$

where G_{contra} and G_{ipsi} are gains for rotation in each direction. Directional preponderance is insensitive to absolute values of gain. As Fig. 2C shows, directional preponderance for the plateau gain remained small and its time course, although noisy, could be fit by the sum of rising and falling exponential functions.

Persistent asymmetry in the dynamic index

Like the VOR (plateau) gain, the dynamic index was asymmetric after a unilateral plug. Although plateau gain became symmetric within 30 days after the plug, dynamic index did not. The dynamic index for contralesional rotation remained higher than that for ipsilesional rotation. In some cases, there was no overlap in the distributions of dynamic index for ipsi- and contralesional rotation. Figure 3A shows typical examples of VOR responses after the plateau gain had recovered. In Fig. 3B–E, the dynamic index, measured 30 days or more postlesion, is plotted against plateau gain for four cats. Three of the cats had unilateral canal plugs, and one [K(LBX)] had a hemilabyrinthectomy. In a fourth cat with a canal plug, D(CP), the results (not shown) were similar to those in Fig. 3. The outcome illustrated in Fig. 3 appeared to be stable. Some of the illustrated data from cat P were obtained between 3 and 4 months after the ca-

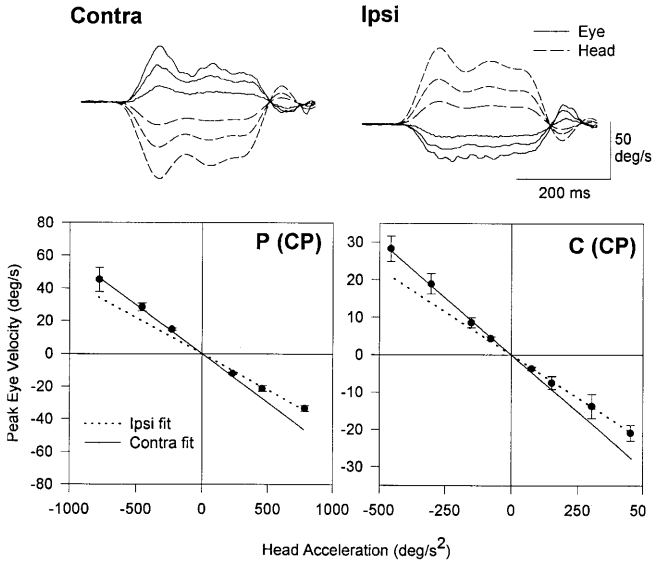

Fig. 4 Response to pulses with varying velocities, after recovery. Traces at the *top* are sample responses to contralesional and ipsilesional pulses, with plateau velocities of 15°/s, 30°/s, and 50°/s, in cat P(CP) 35 days postplug. Lower panels: peak eye velocity as a function of mean head acceleration during the rising phase of the velocity pulse. Ipsilesional head and eye motion are positive. Note different scales for cat P(CP) and cat C(CP). Means and standard deviations are shown. Lines were fit to either ipsi-or contralesional data, then reflected about the *y*-axis for comparison. *n*=9 for cat P(CP) and *n*=10 for cat C(CP)

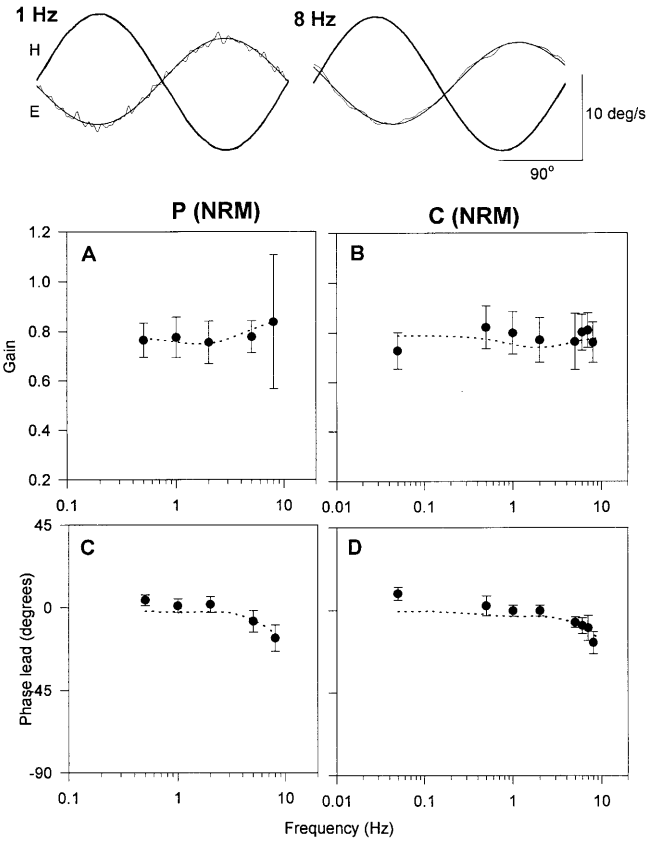

Fig. 5 Frequency response of the normal VOR. Traces at the *top* are head (*H*) and eye (*E*) velocity of cat C(NRM) during sinusoidal rotation at 1 Hz and at 8 Hz. Fitted sinusoids are superimposed on the data. *A*, Gain as a function of frequency for cat P(NRM); *B*, gain vs. frequency for cat C(NRM). Means and standard deviations are shown. *n*=9 for cat P(NRM) and 11 for cat C(NRM). *Dotted lines* are simulations using the model. *C,D* phase angle as a function of frequency for cat P(NRM) and cat C(NRM), respectively

nal plug and showed no further changes. In K(LBX), data obtained up to 80 days postlesion showed a lack of symmetry in either gain or dynamic index.

Several characteristics of the peak and plateau could contribute to the asymmetric dynamic index, including time relative to motion onset, the magnitude of the acceleration, and/or the frequency content of the stimulus. We addressed the first possibility by applying a second acceleration at the end of the plateau in cats P and C. The dynamic index calculated from the second overshoot and plateau were also asymmetric (data not shown). In the following sections, we will show that the asymmetry depended on the frequency of the stimulus but did not depend on the magnitude of the acceleration.

Effect of stimulus velocity and acceleration

If the asymmetry in Fig. 3 is due to a nonlinear response to high-acceleration rotations, the VOR should be symmetric at low pulse velocities and accelerations, but should show signs of saturation for higher velocities toward the plugged side. In Fig. 3, the mean angular acceleration during the rising phase was between 300 and 460°/s^2. In another experiment, we varied the mean acceleration during the rising phase of the velocity pulse from 50 to 750°/s^2. The temporal pattern of the stimulus was constant so that velocity and acceleration covaried. Sample responses from P(CP) at plateau velocities of 15°/s, 30°/s, and 50°/s are shown in Fig. 4 (top). In C(CP), plateau velocity ranged from 5–30°/s. Within the range tested, asymmetry did not depend on stimulus velocity or acceleration. The dynamic index was significantly asymmetric (Student's *t*-test, $P<0.01$) for plateau velocities as low as 10°/s. At 5°/s the mean dynamic index was asymmetric, but we could not demonstrate significance at 5°/s because of a poor signal-to-noise ratio. In Fig. 4 (lower panels), peak eye velocity is plotted as a function of the mean head acceleration during the rising phase for both cats. Linear fits are shown for contralesional rotations (acceleration negative, solid lines) and for ipsilesional rotations (acceleration positive, dotted lines). The lines were reflected across zero to illustrate that the peak eye velocity was higher for contralesional rotation. The slopes of the regression lines for rightward and leftward rotation were significantly different in both cats (Student's *t*-test, $P<0.0005$; *n*=21 for cat P and 38 for cat C). Peak velocity showed no sign of saturation within the range that we tested.

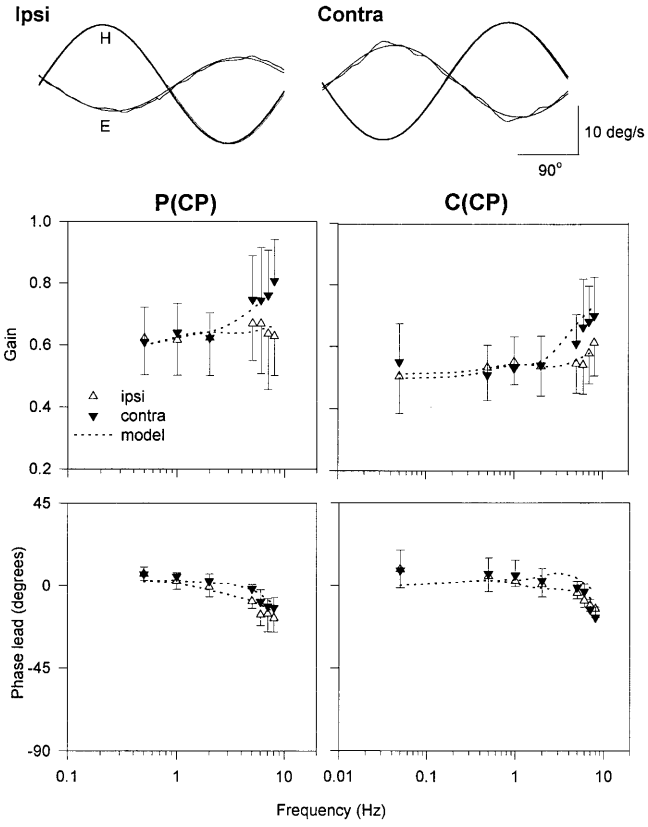

Fig. 6 Frequency-dependent asymmetry after recovery. Traces at the *top* are full cycles reconstructed from half-cycles of ipsi- or contralesional rotation at 8 Hz; examples are from cat P(CP) on day 50 post-plug. *Middle row*, gain as a function of frequency for cat P(CP) and cat C(CP), respectively. *Empty triangles*, data from ipsilesional rotation; *inverted filled triangles*, contralesional rotation. Means and standard deviations are shown. n=22 for cat P(CP) and 12 for cat C(CP). Data were gathered between 30 and 131 days postplug. *Dotted lines* are simulations using the model in Fig. 9. *Bottom row*, phase lag as a function of frequency for cat P(NRM) and cat C(NRM), respectively. Phase leads are positive. Symbols and *error bars* as in *middle row*

Normal and post-plug frequency response of the VOR

We used sinusoidal stimuli to determine whether the asymmetry depended on stimulus frequency. We first measured the frequency response of the normal VOR between 0.05 Hz and 8 Hz. Sample responses at 1 and 8 Hz are shown at the top of Fig. 5. Figure 5A,B shows the mean and standard deviation of VOR gain as a function of frequency in two cats. The gain of the VOR was approximately 0.8 at all frequencies between 0.05 and 8 Hz. Of the two cats, responses in cat C were less variable, probably because amphetamine prevented drowsiness. The dotted lines illustrate the performance of a bilateral model that we used to simulate the data. Details of the model will be given in the Discussion. Figure 5C,D shows that head and eye velocity were approximately in phase up to 2 Hz, but eye velocity lagged head velocity at 5 Hz and above. In the model, a pure delay of 5–7 ms was added to fit the phase data.

After a canal plug, the asymmetry in the VOR recovered for low-frequency but not for high-frequency rotation. Beginning 30 days after the canal plug, we measured the frequency response of the ipsi- and contralesional VOR during half-cycles of sinusoidal rotation. Any bias velocity was rejected by shifting the eye velocity records along the velocity axis (see Materials and methods), so that the asymmetric gain of the VOR could be measured accurately. Figure 6 (top) shows examples of reconstructed full cycles of either ipsilesional or contralesional rotation. The results are summarized in Fig. 6A,B. With increasing stimulus frequency, the ipsilesional gain did not change significantly, but the contralesional gain increased. As a result, the VOR was asymmetric above 2 Hz. The difference between ipsi- and contralesional gains was significant at 5 Hz, 7 Hz, and 8 Hz in cat P(CP) (Student's t-test, P<0.01; n=17). In cat C(CP), the difference was significant at 6 Hz and 8 Hz (t-test, P<0.05; n=12). During contralesional rotation, VOR gain approached normal as stimulus frequency increased from 2 to 8 Hz. At 0.05–1 Hz, there was no significant asymmetry, and the VOR gain was approximately 70% of normal for rotation in both directions. Phase angles are shown for cat P(CP) in Fig. 6C and for C(CP) in Fig. 6D. During contralesional rotation, the phase lag of the VOR was slightly reduced compared with normal, but the difference was not statistically significant.

Comparison of pulse and sinusoid data

If we assume that the VOR's response to *unidirectional* rotation is linear and time-invariant, the frequency components of its response to velocity pulses should match its response to sinusoids. Spectral analysis of velocity pulse data showed measurable energy in both head and eye velocities at harmonics of the fundamental (0.75 Hz or 1.25 Hz). Sample power spectra for head and eye velocities are shown in Fig. 7 (top panels) for leftward rotation in cat P(CP). Head velocity spectra were identical for rightward and leftward rotations. We computed the transfer functions of the VOR, for ipsi-and contralesional rotation, from the cross power spectra of the head and eye velocity signals. Directional preponderances were calculated from the resulting transfer functions and, for comparison, also from the sinusoidal VOR. The directional preponderances for four cats are summarized in Fig. 7. For both stimulus waveforms, the directional preponderance of the VOR increased with increasing stimulus frequency above 1 Hz or 2 Hz.

Residual horizontal VOR function after bilateral plugs

Plugging the horizontal canal resulted in a bony plug that completely occluded the lumen of the canal. However, if the cupula is intact, occlusion of the canal does not prevent responses of primary vestibular afferents to rotation at high frequencies (Rabbitt et al. 1996). To investigate

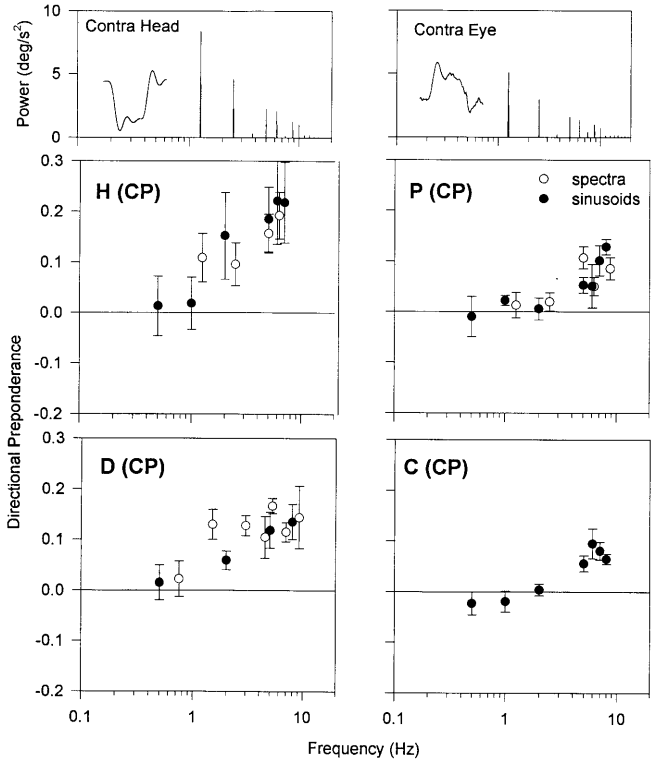

Fig. 7 *Top*: Typical power spectra for head and eye velocity during a contralesional velocity pulse in cat P(CP). *Insets* are the corresponding records in the time domain. *Lower four panels*: Directional preponderances derived from power spectra (*empty symbols*) and from sinusoidal stimuli (*filled symbols*). Each panel shows means of all data from one cat more than 30 days postplug. Error bars are SEMs. Sample sizes: cat H(CP) spectra, 9; cat H(CP) sinusoids, 7; cat P(CP) spectra, 22; cat P(CP) sinusoids, 22; cat D(CP) spectra, 8; cat D(CP) sines, 6; cat C(CP) sinusoids, 12

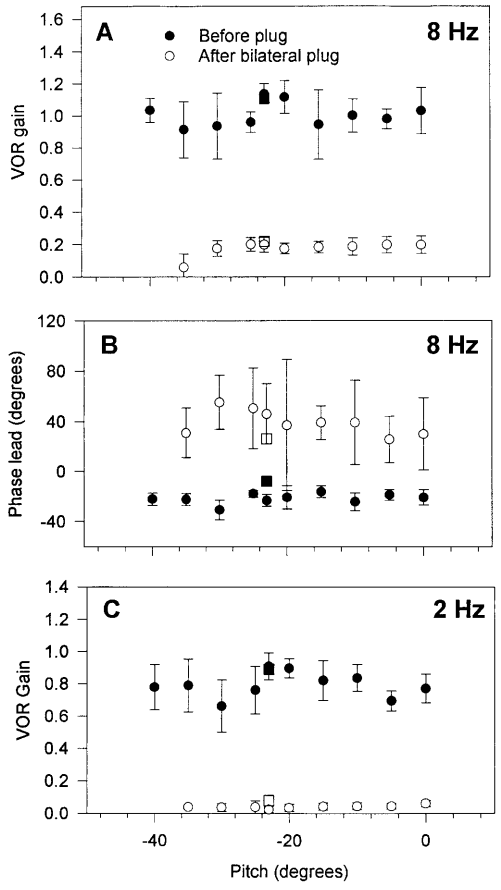

Fig. 8A–C Gain and phase as a function of pitch angle of the head with respect to the axis of rotation. Means and standard deviations are shown. **A** Gain at 8 Hz before and after a bilateral plug. Data from cat G(NRM) (*filled circles*, n=5) and cat G(BCP) (*empty circles*, n=12). **B** Phase angle between head and eye velocity. **C** Gain at 2 Hz before and after the bilateral plug. n=5 before and 12 after the plug. *Squares* are model simulations

such residual responses and, at the same time, to measure any contribution of the vertical canals to the horizontal VOR, we plugged the horizontal canals bilaterally in two cats. The results from cat G are shown in Fig. 8. The position of the cat's head was varied, in the pitch plane, with respect to the (earth vertical) axis of rotation. The pitch angle ranged from the upright position to 40° forward (nose down); forward pitch is negative. The plane of the horizontal canals was estimated to lie at 23° nose down (Blanks et al. 1972). Before the bilateral plug, the gain of the horizontal VOR at 2–8 Hz was not significantly dependent on pitch angle over the range that we used. After the plug, the horizontal VOR at 2 Hz was too small to measure reproducibly (Fig. 8C). At 8 Hz, however, the horizontal VOR had a gain of approximately 0.2 (Fig. 8A). Unlike the normal VOR, the residual response had a mean phase lead of 39° (Fig. 8B). We were unable to demonstrate any significant effect of pitch angle on gain or phase, either at 2 Hz or at 8 Hz. Although preliminary results suggested that the vertical canals may contribute at much lower frequencies (0.25 Hz and less), they did not appear to contribute significantly to the horizontal VOR at 2–8 Hz. Responses showed some tendency to increase over time after the plug, but the trend was not significant. Therefore, responses from 3–35 days postplug were averaged together for Fig. 8. The results of the bilateral plug in cat D were similar for the upright position; pitch angle was not varied in cat D.

Discussion

It has been known for some time that the VOR shows asymmetric responses to high-acceleration, impulsive rotation after unilateral damage (Halmagyi et al. 1993; Tabak and Collewijn 1995; Aw et al. 1996). If the stimulus velocity exceeds approximately 100°/s, asymmetry appears regardless of the stimulus waveform (Baloh et al. 1979; Paige 1983; Fetter and Zee 1989a; Paige 1989; Tusa et al. 1996). Some investigators have observed a slight persistent asymmetry at frequencies higher than 1 Hz (Vibert et al. 1993; Foster et al. 1997), but they did not determine whether the asymmetry was related to fre-

quency *per se* or to peak acceleration. We show here that asymmetric responses to impulsive stimuli can appear at low accelerations and that asymmetric responses to sinusoidal stimuli appear at high frequencies. Response saturation at high stimulus velocities is one source of persistent asymmetry (Paige 1983; Fetter and Zee 1989a) but it does not account for our results. The high-frequency asymmetry is also distinct from bias velocity (Paige 1983, 1989).

Signals originating from the vertical canals

Unless the axis of rotation lies parallel to the planes of the anterior and posterior semicircular canals, vertical canals will contribute part of the signal that drives the horizontal VOR at low frequencies. This cross-coupling between the vertical and horizontal VOR compensates for the slightly different geometries of the semicircular canals and the extraocular muscles (Robinson 1982a). After both horizontal canals are plugged, the vertical canals generate a small but consistent horizontal response, depending on pitch position, at frequencies up to 1 Hz (Baker et al. 1982; Yakushin et al. 1995; Angelaki and Hess 1996); upright, the response is large enough to measure. Our results suggest that at 2 Hz the vertical canals do not generate a measurable horizontal VOR in the upright position. Our failure to observe cross-coupling was probably due to the relatively high frequencies of rotation; at lower frequencies, responses could be obtained, as in the earlier reports. Further investigation is needed to fully understand the relationship between stimulus frequency and the degree of cross-coupling between the vertical canals and the horizontal VOR. For our purposes here, the results suggest that the contribution of the vertical canals to the horizontal VOR at 2 Hz and more after a unilateral plug can probably be ignored.

Neural and mechanical factors in the VOR's frequency response

After a unilateral plug, the horizontal VOR gain reached its asymptotic value for rotation in both directions within the first 3 postoperative weeks. This was consistent with earlier results in the same species (Courjon et al. 1977; Maioli et al. 1983). However, dynamic symmetry did not recover, at least during the first 5 months postplug. The reason for this is uncertain. In human patients with unilateral damage, the VOR responds poorly to sudden acceleration toward the deafferented side (Halmagyi et al. 1993), possibly because primary afferents on the intact side respond linearly only within a limited range of stimulus velocities. However, in our cats, the persistent asymmetry was independent of acceleration and velocity, suggesting that the accelerations we used were small enough that most or all of the primary vestibular afferents on the intact side could follow the stimulus waveform. This would be consistent with the known physiology of primary afferents (Goldberg and Fernandez 1971a; Fernandez and Goldberg 1971). A subpopulation of primary vestibular afferents shows a consistently larger response to ipsilateral than contralateral rotation (Fernandez and Goldberg 1971). This "linear asymmetry" was not reported to depend on the magnitude of the stimulus or on its frequency, although high-frequency sinusoids were used (Fernandez and Goldberg 1971). If it were combined with frequency-dependent signal processing in the VOR pathway, the linear asymmetry might explain the persistent asymmetry in the VOR above 5 Hz. This possibility will be explored in simulations of the VOR.

For some primary vestibular afferents, the sensitivity of firing rate to head velocity increases with frequency between 1 and 8 Hz and firing rate leads head velocity (Goldberg and Fernandez 1971b; Keller 1976; Louie and Kimm 1976). The phase lead is thought to contribute significantly to the responses of secondary neurons (Anastasio 1994). If the high-frequency responses of contralesional primary afferents were selectively amplified during learning, they might account for the high-frequency gain enhancement that we observed for contralesional rotation. Based on this idea, the model will include a separate afferent pathway that contains a high-pass filter.

Another possible source of high-frequency gain enhancement is the plugged canal. At 8 Hz (but not at 2 Hz), we obtained a small but significant horizontal response after a bilateral horizontal canal plug. The response had a mean phase lead of 39.5°, compared with a lag of 21.5° before the plug in the same cat; i.e., a bilateral plug adds a phase lead of +61° at 8 Hz. This value is close to the cupular phase lead of 57° predicted for a plugged canal by the model of Rabbitt et al. (1996, and personal communication). At 2 Hz, the plugged canals did not generate a detectable signal. Accordingly, the model will represent the plugged canal as a high-pass filter with a gain element.

The recovery of VOR gain is thought to utilize changes in the efficacy of transmission by the commissural network that interconnects the bilateral vestibular nuclei (Dieringer and Precht 1979a,b; Galiana et al. 1984; Galiana 1986). Ipsilesional secondary neurons recover some sensitivity to head velocity signals (Hamman and Lannou 1988; Newlands and Perachio 1990; Precht et al. 1966), and the commissure is one source of such signals. Transmission by the commissure may contribute selectively to the VOR at middle and low frequencies (de Jong et al. 1980; Cheron 1990; Anastasio and Robinson 1991). In one bilateral model the commissure is part of a network that also includes low-pass filters (Galiana and Outerbridge 1984). An alternative configuration places the filter in the commissure itself. Limitations in the frequency response of commissural transmission combined with unilateral damage could result in frequency-dependent asymmetry in the responses of secondary neurons. Although the projections from secondary neurons to motoneurons are bilateral, the crossed and uncrossed

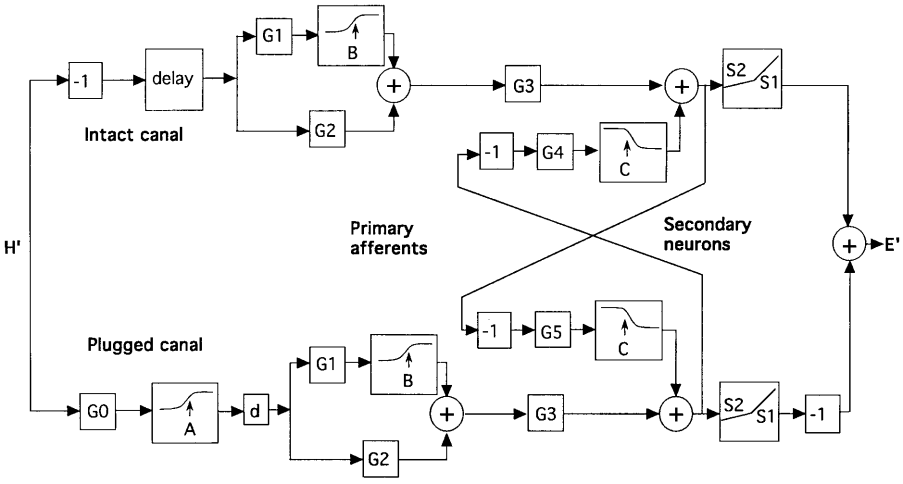

Fig. 9 A bilateral model of the VOR. *H'* represents angular head velocity. *Uncrossed pathway*: ***G3*** is the gain of the direct input from primary afferents to vestibular neurons. *Commissural pathway*: *G4* and *G5* are the gains of the crossed pathways. The projection across the commissure is associated with a change in the sign (–1). *C* is the cutoff frequency of the vestibular commissure, *S1*, *S2* are the gains of secondary neurons for increases and decreases in firing, respectively, *G0* is the gain of the plugged canal (either 1 or 0), *d* is a pure delay, *G1* and *G2* are ains of two groups of primary afferents, *B* is the cutoff frequency of primary afferents with high-frequency gain enhancement

Table 1 Values of the model parameters that were used to simulate our data; see Fig. 9 for definitions of the parameters. Static variables were adjusted to fit normal data, but were not readjusted to fit compensated data from the same cat. Modified variables were readjusted (*NRM* normal data, *CP* after recovery from a unilateral plug, *BCP* bilateral plug, *NE* changing this parameter had no effect under the particular conditions indicated, *NI* parameter not included in model)

	P (NRM)	P (CP)	C (NRM)	C (CP)	G (NRM)	G (BCP)
Static variables						
Delay (ms)	7	7	5	5	7	7
A (Hz)	NI	7.0	NI	7.0	NI	7.0
G_2	0.58	0.58	0.58	0.58	0.56	0.56
B (Hz)	4.0	4.0	3.5	3.5	4.0	4.0
C (Hz)	1.5	1.5	1.15	1.15	2.0	2.0
Modified variables						
G_0	1	0.1	1	0.1	1	0.1
G_1	0.18	1.70	0.08	2.10	0.5	1.0
G_3	1.15	0.62	1.20	0.49	1.10	2.00
G_4	0.15	0.40	0.12	0.60	0.30	1.00
G_5	0.15	1.60	0.12	1.60	0.30	1.00
S_1	NE	0.55	NE	0.57	NE	NE
S_2	NE	0.45	NE	0.43	NE	NE

projections are unequal in strength (Scudder and Fuchs 1992; Broussard et al. 1995), so that asymmetry would probably appear in the VOR.

Simulations of the VOR

We simulated the horizontal VOR using a simple bilateral model (Fig. 9). In our model, the bilateral VOR circuitry is interconnected by recurrent commissural pathways, a feature of other bilateral VOR models (Galiana and Outerbridge 1984; Galiana 1986). Recurrent commissural connections allowed all of the inputs to secondary neurons to converge at a single summation point. Versions of the model that included only feedforward commissural pathways also could simulate our results, provided that low-pass filtering was a feature of the commissural pathway. We made no attempt to include all of the functional groups of neurons in the VOR pathway. In order to keep the model simple, we also omitted several well-known features of VOR processing that are important at lower frequencies, such as the limited frequency response of primary afferents, velocity storage (Raphan et al. 1979), neural integration, and interactions with other oculomotor control systems (Robinson 1982b).

In Fig. 9, the plugged canal was represented by a gain (G_0) and a high-pass filter with a rolloff frequency of A. For a bilateral plug, these features were present on both sides. To simulate the normal VOR, the high-pass filter was omitted, and G_0 was 1. The latency of the VOR was represented by a pure delay (*d*). G_1 and G_2 were gains of parallel pathways that received input from each horizontal canal. The G_1 pathway included a high-pass filter with a rolloff frequency, *B*. All filters in the model were virtual Bessell filters with linear phase (National Instruments). Commissural pathways (G_4, G_5) included low-pass filters with rolloff frequency *C*. On both sides of the model, the responses of secondary neurons were assumed to be nonlinear, with larger responses to excitatory than to inhibitory inputs (S_1, S_2). This property was based on published observations that the responses of brainstem VOR interneurons are asymmetric (Lisberger and Miles 1981; Lisberger et al. 1994). Although the responses of some primary afferents also are nonlinear, we found that to simulate our data, we had to place a nonlinear element downstream of the commissural network. Placing the nonlinear element upstream resulted in

asymmetric responses at all frequencies. However, some combination of upstream and downstream nonlinearities might also be successful.

The parameters of the model (shown in Table 1) were first optimized during simulations of the normal VOR in each cat (NRM in Table 1). Bode plots of these simulations were shown in Fig. 5 (dotted lines). To determine how best to represent the effect of plugging on canal dynamics, we next simulated the bilateral plug. The central filters (*B* and *C*) were not changed during this second optimization, but G_0, *A*, and the central gains were all adjusted. The simulated gain and phase before and after the bilateral plug are shown in Fig. 8 (squares) and the values of model parameters are shown in Table 1 (BCP).

We used several configurations of the model in attempts to simulate the dynamic asymmetry after a unilateral plug. These included (1) the configuration in Fig. 9, (2) placing the nonlinearity upstream of the commissures, and (3) eliminating central filters and generating the high-frequency gain enhancement at the plugged canal. In case 3 it was impossible to selectively enhance high-frequency responses for rotation away from the plugged side. For the configuration in Fig. 9, all gains were adjusted to optimize the fit to the VOR after recovery. G_1 was increased selectively to simulate the high-frequency gain enhancement after recovery; increasing G_0 generated high-frequency enhancement but the asymmetry had the wrong polarity. To adjust the gain and symmetry at low frequencies, we increased or decreased the commissural gains, G_4 and G_5. Bode plots of the simulations are shown in Fig. 6, and parameter values are in Table 1 (CP).

Based on our model simulations, we suggest that the frequency-dependent asymmetry after a unilateral canal plug or labyrinthectomy could be due to properties of the central VOR pathways. The commissural network is thought to contribute to the VOR primarily at mid-to-low stimulus frequencies (de Jong et al. 1980; Cheron 1990; Anastasio and Robinson 1991). If the changes underlying recovery of symmetry occur largely in the commissural inputs to vestibular neurons, the responses of VOR interneurons on the plugged side would depend in part on the commissure. The limited frequency response of the commissural network could prevent recovery of symmetry at high frequencies by limiting the frequency response of the interneurons on the plugged side. In our model, the low-pass filter in the commissure permitted symmetric responses at low frequencies while preserving asymmetric responses at high frequencies. Further experimentation is required to determine whether, in the VOR control system, a similar mechanism prevents full recovery of symmetry in the high-frequency VOR.

Acknowledgements. We thank J. Hong for participating in some of the experiments, Drs. J. Baker, R. Rabbitt and R. D. Tomlinson for helpful discussions, and Drs. S. du Lac and J. L. Raymond for their comments on an earlier version of this paper. This research was supported by an operating grant (MRC:MT-12254) from the Medical Research Council of Canada.

References

Anastasio TJ (1994) The fractional-order dynamics of brainstem vestibulo-oculomotor neurons. Biol Cybern 72:69–79

Anastasio TJ, Robinson DA (1991) Failure of the oculomotor neural integrator from a discrete midline lesion between the abducens nuclei in the monkey. Neurosci Lett 127:82–86

Angelaki DE, Hess, BJM (1996) Adaptation of primate vestibulo-ocular reflex to altered peripheral vestibular inputs. II. Spatio-temporal properties of the adapted slow phase eye velocity. J Neurophysiol 76:2954–2971

Aw ST, Halmagyi, GM, Haslwanter, T, Curthoys, IS, Yavor, RA, Todd, MJ (1996) Three-dimensional vector analysis of the human vestibuloocular reflex in response to high-acceleration head rotations. II. Responses in subjects with unilateral vestibular loss and selective semicircular canal occlusion. J Neurophysiol 76:4021–4030

Baker J, Goldberg, J, Peterson, B, Schor, R (1982) Oculomotor reflexes after semicircular canal plugging in cats. Brain Res 252:151–155

Baloh, RW, Sills, AW, Honrubia, V (1979) Impulsive and sinusoidal rotatory testing: a comparison with result of caloric testing. Laryngoscope 89:646–654

Blanks RHI, Curthoys IS, Markham CH (1972) Planar relationships of semicircular canals in the cat. Am J Physiol 223:55–62

Broussard DM, Bhatia JK (1994) Effects of blockade of NMDA receptors and unilateral vestibular damage on the dynamics of the VOR. Neurosci Abstr 20:1191

Broussard DM, deCharms RC, Lisberger SG (1995) Inputs from the ipsilateral and contralateral vestibular apparatus to behaviorally-characterized abducens neurons in rhesus monkeys. J Neurophysiol 74:2445–2459

Broussard DM, Bhatia JK (1996) The physiological basis of imperfect compensation by the VOR at high frequencies of rotation. Ann NY Acad Sci 781:585–588

Cheron G (1990) Effect of incisions in the brainstem commissural network on the short-term vestibulo-ocular adaptation of the cat. J Vestib Res 1:223–239

Cirelli C, Pompeiano M, D'Asciano P, Pompeiano O (1993) Early c-fos expression in the rat vestibular and olivo cerebellar systems after unilateral labyrinthectomy. Arch Ital Biol 131:71–74

Courjon JH, Jeannerod M, Ossuzio I, Schmid R (1977) The role of vision in compensation of vestibulo ocular reflex after hemilabyrinthectomy in the cat. Exp Brain Res 28:235–248

Dieringer N, Precht W (1979a) Mechanisms of compensation for vestibular deficits in the frog. I. Modification of the excitatory commissural system. Exp Brain Res 36:311–328

Dieringer N, Precht W (1979b) Mechanisms of compensation for vestibular deficits in the frog. II. Modification of inhibitory pathways. Exp Brain Res 36:329–341

Fernandez C, Goldberg JM (1971) Physiology of peripheral neurons innervating semicircular canals of the squirrel monkey. II. Response to sinusoidal stimulation and dynamics of peripheral vestibular systems. J Neurophysiol 34:661–675

Fetter M, Zee DS (1989a) Recovery from unilateral labyrinthectomy in rhesus monkey. J Neurophysiol 59:370–393

Fetter M, Zee DS (1989b) Effect of lack of vision and of occipital lobectomy upon recovery from unilateral labyrinthectomy in rhesus monkey. J Neurophysiol 59:394–407

Fetter M, Zee DS, Koenig E, Dichgans J (1990) Head-shaking nystagmus during vestibular compensation in humans and rhesus monkeys. Acta Otolaryngol 110:175–181

Foster CA, Demer JL, Morrow MJ, Baloh RW (1997) Deficits of gaze stability in multiple axes following unilateral vestibular lesions. Exp Brain Res 116:501–509

Gacek RR, Schoonmaker J, Lyon MJ (1992) Ultrastructural changes in contralateral superior vestibulo-ocular neurons one year after vestibular neurectomy in the cat. Acta Otolaryngol [Suppl] 495:5–15

Galiana HL (1986) A new approach to understanding adaptive visual-vestibular interactions in the central nervous system. J Neurophysiol 55:349–374

Galiana HL, Outerbridge JS (1984) A bilateral model for central neural pathways in vestibuloocular reflex. J Neurophysiol 51:210–241

Galiana HL, Flohr H, Melvill Jones G (1984) A reevaluation of intervestibular nuclear coupling: its role in vestibular compensation. J Neurophysiol 51:242–259

Goldberg JM, Fernandez C (1971a) Physiology of peripheral neurons innervating semicircular canals of the squirrel monkey. I. Resting discharge and response to constant angular accelerations. J Neurophysiol 34:635–660

Goldberg JM, Fernandez C (1971b) Physiology of peripheral neurons innervating semicircular canals of the squirrel monkey. III. Variation among units in their discharge properties. J Neurophysiol 34:676–684

Gonshor A, Melvill Jones G (1973) Changes of human vestibulo-ocular response induced by vision-reversal during head rotation (abstract). J Physiol (Lond) 234:102P

Halmagyi GM, Curthoys IS, Aw ST, Todd MJ (1993) The human vestibulo-ocular reflex after unilateral vestibular deafferentation: the results of high-acceleration impulsive testing. In: Barber HO, Sharpe JA (eds) The vestibulo-ocular reflex and vertigo. Raven, New York, pp 45–54 1993

Hamman K, Lannou J (1988) Dynamic characteristics of vestibular nuclear neurons responses to vestibular and optokinetic stimulation during vestibular compensation in the rat. Acta Otolaryngol [Suppl] 446:1–19

Ito M (1972) Neural design of the cerebellar motor control system. Brain Res 40:81–84

Jensen DW (1983) Survival of function in the deafferentated vestibular nerve. Brain Res 273:175–178

Jong JMBV de, Cohen B, Matsuo V, Uemura T (1980) Midsagittal pontomedullary brain stem section: effects on ocular adduction and nystagmus. Exp Neurol 68:420–442

Keller EL (1976) Behavior of horizontal semicircular canal afferents in alert monkey during vestibular and optokinetic stimulation. Exp Brain Res 24:459–471

Lisberger SG, Miles FA (1981) Role of primate medial vestibular nucleus in long-term adaptive plasticity of vestibulo-ocular reflex. J Neurophysiol 45:869–890

Lisberger SG, Pavelko TA (1986) Vestibular signals carried by pathways subserving plasticity of the vestibulo-ocular reflex in monkeys. J Neurosci 6:346–354

Lisberger SG, Pavelko TA, Broussard DM (1994) Responses during eye movements of brainstem neurons that receive monosynaptic inhibition from the flocculus and ventral paraflocculus in monkeys. J Neurophysiol 72:909–927

Louie AW, Kimm J (1976) The response of 8th nerve fibers to horizontal sinusoidal oscillations in the alert monkey. Exp Brain Res 24:447–457

Maioli C, Precht W, Reid S (1983) Short- and long-term modifications of vestibulo-ocular response dynamics following unilateral vestibular nerve lesions in the cat. Exp Brain Res 50: 259

Miles FA, Evarts EV (1979) Concepts of motor organization. Annu Rev Psychol 30:327–362

Newlands SD, Perachio AA (1990) Compensation of horizontal canal related activity in the medial vestibular nucleus following unilateral labyrinth ablation in the decerebrate gerbil. Exp Brain Res 82:359–372

Paige GD (1983) Vestibulo-ocular reflex and its interactions with visual following mechanisms in the squirrel monkey. II. Response characteristics and plasticity following unilateral inactivation of horizontal canal. J Neurophysiol 49:152–168

Paige GD (1989) Nonlinearity and asymmetry in the human vestibulo-ocular reflex. Acta Otolaryngol 108:1–8

Precht W, Shimazu H, Markham CH (1966) A mechanism of central compensation of vestibular function following hemilabyrinthectomy. J Neurophysiol 29:996–1010

Rabbitt RD, Boyle R, Yamauchi A, Highstein SM (1996) A residual end organ response persists following semicircular canal plugging in the toadfish, *Opsanus tau*. Soc Neuroscience Abstr 22:1819

Racine RJ, Wilson DA, Gingell R, Sunderland D (1986) Long-term potentiation in the interpositus and vestibular nuclei in the rat. Exp Brain Res 63:158–162

Raphan T, Matsuo V, Cohen B (1979) Velocity storage in the vestibulo-ocular reflex arc. Exp Brain Res 35:229–248

Robinson DA (1982a) The use of matrices in analyzing the three-dimensional behavior of the vestibulo-ocular reflex. Biol Cybern 46:53–66

Robinson DA (1982b) A model of cancellation of the vestibulo-ocular reflex. In: Lennerstrand G, Zee DS, Keller EL (eds) Functional basis of ocular motility disorders. Pergamon, New York, pp 5–13

Scudder CA, Fuchs AF (1992) Physiological and behavioral identification of vestibular nucleus neurons mediating the horizontal vestibuloocular reflex in trained rhesus monkeys. J Neurophysiol 68:244–264

Tabak S, Collewijn H (1995) Evaluation of the human vestibulo-ocular reflex at high frequencies with a helmet, driven by reactive torque. Acta Otoloaryngol [Suppl] 520:4–8

Tusa RJ, Grant MP, Buettner UW, Herdman SJ, Zee DS (1996) The contribution of the vertical semicircular canals to high-velocity horizontal vestibulo-ocular reflex (VOR) in normal subjects and patients with unilateral nerve section. Acta Otolaryngol 116:507–512

Vibert G, Waele C de, Escudero M, Vidal PP (1993) The horizontal vestibulo-ocular reflex in the hemilabyrinthectomized guinea-pig. Exp Brain Res 97:263–273

Yakushin S, Dai M, Suzuki J-I, Raphan T, Cohen B (1995) Semicircular canal contributions to the three-dimensional vestibulo-ocular reflex: A model-based approach. J Neurophysiol 74: 2722–2738

Yamane H, Nakagawa T, Iguchi H, Shibata S, Takayama M, Nishimura K, Nakai Y (1995) In vivo regeneration of vestibular hair cells of guinea pig. Acta Otolaryngol [Suppl] 520:174–177